HHS Public Access

Author manuscript

Free Radic Biol Med. Author manuscript; available in PMC 2020 August 25.

Published in final edited form as:

Free Radic Biol Med. 2016 April ; 93: 94–109. doi:10.1016/j.freeradbiomed.2016.02.002.

Up-regulation of Nrf2 is involved in FGF21 mediated fenofibrate protection against type 1 diabetic nephropathy

Yanli Cheng[a,b,c], **Jingjing Zhang**[c,d,e], **Weiying Guo**[a], **Fengsheng Li**[f], **Weixia Sun**[a], **Jing Chen**[c], **Chi Zhang**[b,g], **Xuemian Lu**[g], **Yi Tan**[b,c,g,h], **Wenke Feng**[h,i], **Yaowen Fu**[a], **Gilbert C. Liu**[j], **Zhonggao Xu**[a,*], **Lu Cai**[b,c,g,h,**]

[a]The First Hospital of Jilin University, Changchun 130021, China

[b]The Chinese–American Research Institute for Diabetic Complications, Wenzhou Medical University, Wenzhou 325035, China

[c]Kosair Children's Hospital Research Institute, Department of Pediatrics, University of Louisville, Louisville, KY 40202, USA

[d]Department of Cardiology at the First Hospital of China Medical University, Shenyang 110016, China

[e]Department of Cardiology at the People's Hospital of Liaoning Province, Shenyang 110016, China

[f]The Second Artillery General Hospital, Beijing 100088, China

[g]The Third Affiliated Hospital of the Wenzhou Medical University, Ruian 325200, China

[h]Department of Pharmacology and Toxicology, University of Louisville, Louisville, KY 40202, USA

[i]Department of Medicine, University of Louisville, Louisville, KY 40202, USA

[j]Child and Adolescent Health Research Design and Support, University of Louisville, Louisville, KY 40204, USA

Abstract

The lipid lowering medication, fenofibrate (FF), is a peroxisome proliferator-activated receptor-alpha (PPARα) agonist, possessing beneficial effects for type 2 diabetic nephropathy (DN). We investigated whether FF can prevent the development of type 1 DN, and the underlying mechanisms. Diabetes was induced by a single intraperitoneal injection of streptozotocin in C57BL/6J mice. Mice were treated with oral gavage of FF at 100 mg/kg every other day for 3 and 6 months. Diabetes-induced renal oxidative stress, inflammation, apoptosis, lipid and collagen

*Correspondence to: Department of Nephrology, The First Hospital of Jilin University, 71 Xinmin Street, Changchun 130021, Jilin Province, China. renalxu@163.com (Z. Xu). **Correspondence to: Kosair Children's Hospital Research Institute, University of Louisville, 570 South Preston Street, Baxter I, Suite 304F, Louisville, KY 40202, USA. L0cai001@louisville.edu (L. Cai).

Contribution statement

Y.C. performed the research, contributed to, and analyzed the data. J.Z. set up the type 1 mouse model. W.G., F.L., W.S., J.C. and C. Z. participated in data collection and analysis. X.L., Y.T., W.F., Y.F., G. C.L., Z.X. and L.C. contributed to the initial and consequent project discussion, manuscript discussion, and revision. Z.X. and L.C. participated in the project design, manuscript draft preparation, and revision. All the authors approved the final version of the manuscript.

Conflict of interest

No potential conflicts of interest relevant to this article were reported.

accumulation, and renal dysfunction were accompanied by significant decrease in PI3K, Akt, and GSK-3β phosphorylation as well as an increase in the nuclear accumulation of Fyn [a negative regulator of nuclear factor (erythroid-derived 2)-like 2 (Nrf2)]. All these adverse effects were significantly attenuated by FF treatment. FF also significantly increased fibroblast growth factor 21 (FGF21) expression and enhanced Nrf2 function in diabetic and non-diabetic kidneys. Moreover, FF-induced amelioration of diabetic renal damage, including the stimulation of PI3K/Akt/GSK-3β/Fyn pathway and the enhancement of Nrf2 function were abolished in FGF21-null mice, confirming the critical role of FGF21 in FF-induced renal protection. These results suggest for the first time that FF prevents the development of DN via up-regulating FGF21 and stimulating PI3K/Akt/GSK-3β/Fyn-mediated activation of the Nrf2 pathway.

Keywords

Diabetic nephropathy; PPARα agonist; FGF21; Nrf2; Type 1 diabetes; Oxidative stress; Antioxidants

1. Introduction

Diabetic nephropathy (DN) is one of the microvascular morbidities of diabetes and a major cause of mortality. Oxidative stress is an important pathogenic factor in the development and progression of DN [1]; therefore, molecules regulating renal anti-oxidative stress, such as nuclear factor (erythroid-derived 2)-like 2 (Nrf2), are potentially important targets for lowering the risk of DN [2]. Nrf2 is a transcription factor that controls the cellular defense against oxidative stress [2,3]. Nrf2 is normally sequestered by Kelch-like ECH-associated protein 1 (Keap1) in the cytoplasm, and Keap1 is responsible for promoting its proteasomal degradation [2,3]. Once Nrf2 is released from Keap1, translocates into the nucleus, and binds antioxidant response element (ARE), it can turn on the transcription of antioxidant genes, including heme oxygenase-1 (HO-1) and NAD(P)H: quinone oxidoreductase 1 (NQO1). In line with these findings, stimulating Nrf2 function might represent a promising strategy for prevention DN [2–6].

Given the potential risk of introducing adverse effects by new drugs, the application of existing medications originally approved for treating other diseases may offer a more rational approach for treating diabetic complications [7,8]. Fenofibrate (FF) is a peroxisome proliferator-activated receptor-alpha (PPARα) agonist with lipid-lowering property, and is in use for about three decades. There is evidence suggesting that FF is protective against DN in type 2 diabetic patients [9]. Another study using db/db mouse models also demonstrated that FF ameliorated diabetic renal damage through the improvement of renal lipid profile [10]. The potential for FF as a therapeutic approach for renal damages induced by diabetes is supported by the finding that FF could prevent doxorubicin (DOX)-induced renal damage mediated by oxidative stress [11,12]. It has been confirmed that the effect of FF on diabetic renal damages is independent of its lipid-lowering ability [13–15]. However, studies that address the mechanisms through which FF ameliorates renal damage from type 1 diabetes are few.

It has been reported that fibroblast growth factor 21 (FGF21) is transcriptionally regulated by PPARα, and FF increases plasma levels and the organ expressions of FGF21. Furthermore, FGF21 can decrease organ damages through various mechanisms [16–19], including an anti-oxidative effect through the up-regulation of Nrf2, thereby preventing inflammation, cell death, and hypertrophy not associated with dyslipidemia [16,17]. These findings prompt us to explore whether FF stimulates FGF21 up-regulation, activates Nrf2, and protects the kidney from diabetic injuries. We employed a streptozotocin (STZ)-induced diabetic mouse model as reported before [20–22]. We examined renal function changes, histopathologic, and biochemical alterations at 3 and 6 months after the onset of diabetes. To establish the role of FGF21, we further assessed FF-induced renal protection from type 1 diabetes injury in mice with FGF21 gene deletion (FGF21-null mice).

2. Materials and methods

2.1. Animals

FGF21-null mice with C57BL/6J background were given as a gift by Dr. Steve Kliewer (University of Texas Southwestern Medical Center, Dallas, TX, USA). Eight-week-old, male FGF21-null mice with age- and gender-matched C57BL/6J mice were used in the present study. All mice were housed at 22 °C with a 12:12-h light–dark cycle and allowed free access to standard chow and tap water in the University of Louisville Research Resources Center. All procedures were approved by the Institutional Animal Care and Use Committee of the University of Louisville, certified by the American Association for Accreditation of Laboratory Animal Care.

2.2. The model of type 1 diabetes

Based on our previous experiences [20–22], type 1 diabetes were induced with a single intraperitoneal dose of STZ (Sigma-Aldrich, St. Louis, MO, USA) dissolved in 0.1 M sodium citrate buffer (pH 4.5) at 150 mg/kg. Control animals received the same volume of citrate buffer. Three days after injection, hyperglycemia (blood glucose levels ≥ 250 mg/dl) was noted in STZ-injected mice. Diabetic and control mice were randomly divided into two groups, with or without FF (Sigma-Aldrich; dissolved in 1% sodium carboxyl methylcellulose [Na-CMC] or 1% Na-CMC) treatment (100 mg/kg by oral gavage, every other day). At experimental end, mice were euthanized and blood, urine, and kidney were harvested for protein, mRNA, and histopathologic analysis.

The first part of this study was designed to study the effect of FF on DN, in which C57BL/6J mice were randomly allocated to four groups (n=12 per group): control (Ctrl), FF, DM, and DM with FF treatment (DM/FF). At the end of FF treatment 3 months later (3 M), five in each group were euthanized. The derivation of animal number was based on the statistical power requirement calculated in our previous studies [20–22]. Other mice continued to receive FF for an additional 3 months (6 M totally).

The second part of this study was designed to investigate whether the prevention of type 1 DN by FF depends upon FGF21. FGF21-null and their wild type (WT) control were

randomly divided into Ctrl, FF, DM, and DM/FF groups. At the end of FF treatment (3 M), mice were euthanized for organ harvest and further analysis.

2.3. Urine albumin to creatinine ratio assay

At each time point, spot urine was collected from the mice using clean Wide-Mouth Straight-Sided PMP Jars (Thermo Scientific, NY, USA) using bladder palpation. Urine samples were discarded if contamination by feces, food, or water was noted; samples were kept frozen at −20 °C until analysis [22–25]. Urinary albumin-to-creatinine ratio (UACR) was measured to evaluate renal function [22–25], and urine albumin, creatinine were measured according to manufacturers' protocol (Bethyl Laboratories, Montgomery, TX, USA; and BioAssay Systems, Hayward, CA, USA), respectively. The ratio was calculated as by dividing urine albumin to urine creatinine (μg/mg).

2.4. Renal histopathologic examination and immunofluorescence staining

Kidney tissues were fixed in 10% formalin for 24 h, embedded in paraffin, and sectioned at 5 μm thickness for pathological examination and immunofluorescent staining. The sections were deparaffinized and rehydrated, stained with hematoxylin and eosin (H&E). Periodic acid-Schiff (PAS) staining was used to examine the glycogen content of renal tissues, as described previously [25]. Renal fibrosis was evaluated by Sirius-red and Masson's staining for collagen [22,26]. Briefly, sections were stained with mixture of 0.1% Sirius Red F3BA and 0.25% Fast Green FCF. We used the Sigma-Aldrich Trichrome Staining Kit for Masson's staining.

Standard immunofluorescent staining protocols were performed according to previous studies [27]. Anti-Nrf2 antibody (1:400 dilution, Santa Cruz Biotechnology, Dallas, TA, USA) and anti-Fyn antibody (1:400 dilution, Cell Signaling Technology, Boston, MA, USA) were used, and the secondary antibodies Cy3-conjugated immunoglobulin G (IgG; 1:200 dilution, Abcam, Cambridge, MA, USA) were applied for 1 h and counterstained with 4,6-diamidino-2-phenylindole (DAPI; 1:2000 dilution, Sigma-Aldrich) for 10 min at the room temperature. The slices were covered with aqueous mounting medium (Sigma-Aldrich) and analyzed under a fluorescence microscope (Nikon, Tokyo, Japan). All sections were evaluated using a Nikon Eclipse E600 microscopy system.

2.5. Western blot assay

Western blot was performed as previous studies [20]. Kidney tissues were homogenized in RIPA lysis buffer (Santa Cruz Biotechnology) for obtaining total proteins. Nuclear proteins were extracted using a nuclei-isolation kit (Sigma-Aldrich) [28]. Proteins were collected by centrifuging at 12,000 rpm at 4 °C. The total and nuclear proteins were separated on 10% sodium dodecyl sulfate polyacrylamide gel electrophoresis (SDS-PAGE) and transferred to nitrocellulose membranes (Bio-Rad, Hercules, CA, USA). Membranes were blocked with 5% non-fat milk or 0.5% BSA for 1 h, incubated overnight at 4 °C with primary antibodies. The primary antibodies against connective tissue growth factor (CTGF, 1:500 dilution), Nrf2 (1:1000 dilution), histone H3 (1:10,000 dilution), and β-actin (1:3000 dilution) were purchased from Santa Cruz Biotechnology. The following primary antibodies were purchased from Cell Signaling Technology and used at a dilution of 1:1000, including total

PI3K (*t*-PI3Kp85) and phosphorylated PI3K [*p*-PI3Kp85 (Tyr458)/p55 (Tyr199)]; *t*-Akt and *p*-Akt (Ser473); *t*-GSK-3β and *p*-GSK-3β(Ser9); Fyn, Bax, Bcl-2, cleaved-caspase-3, and transforming growth factor (TGF)-β1. Other primary antibodies used were as follows: 3-nitrotyrosine (3-NT, 1:2000 dilution, Millipore, Billerica, MA, USA), 4-hydroxy-2-nonenal (4-HNE, 1:4000 dilution, Alpha Diagnostic International, San Antonio, TX, USA), plasminogen activator inhibitor type 1 (PAI-1, 1:3000 dilution, BD Biosciences, San Jose, CA, USA), tumor necrosis factor-alpha (TNF-α,1:500 dilution, Abcam), and FGF21 (1:2000 dilution, Antibody & Immunoassay Services, University of Hong Kong, China).

After three times of wash with Tris-buffered saline containing 0.05% Tween 20, membranes were incubated with the horseradish peroxidase (HRP)-conjugated secondary antibody (Santa Cruz Biotechnology) for 1 h at room temperature. Bands were visualized using an enhanced chemiluminescence kit (ECL, Thermo Fisher Scientific, Waltham, MA, USA), and quantitative densitometry was performed using Image Quant 5.2 software.

2.6. Quantitative real-time PCR (qRT-PCR)

Kidney samples were frozen and stored at −80 °C. Total RNA was extracted using Trizol reagent (RNA STAT 60 Tel-Test Ambion, Austin, TX, USA). Nanodrop ND-1000 spectrophotometer was used for quantifying RNA concentrations and purities. First-strand complimentary DNA (cDNA) was synthesized from total RNA according to the manufacturer's protocol (Promega, Madison, WI, USA). Reverse transcription was performed in a Mastercycler Gradient (Eppendorf, Hamburg, Germany), with 1 g of total RNA in 20 μL solution containing 4 μL 25 mM $MgCl_2$, 4 μL AMV reverse transcriptase 5× buffer, 2 μL dNTP, 0.5 μL RNase inhibitor, 1 μL AMV reverse transcriptase, 1 μL oligo (dT) primer, and nuclease-free water at 42 °C for 50 min and then 95 °C for 5 min. Primers of FGF21 (Mm00840165), Nrf2 (Mm00477784), NQO1 (Mm01253561), HO-1 (Mm00516005), and β-actin (Mm00607939) were purchased from Applied Biosystems (Carlsbad, CA, USA). qRT-PCR was performed in duplicate with a 20 μL solution containing 10 μL TaqMan Universal PCR master mix, 9 μL cDNA, and 1 μL primer, using the ABI 7500 Real-Time PCR system (Life Technologies Corp., Carlsbad, CA, USA). The comparative cycle time (Ct) method was used to determine fold differences between samples, and the amount of target was normalized to β-actin as an endogenous reference ($2^{-\Delta\Delta Ct}$).

2.7. Terminal deoxynucleotidyl transferase-mediated dUTP nick end labeling (TUNEL) assay

Kidney sections were deparaffinized using xylene and ethanol dilutions, rehydrated, and stained for TUNEL with an ApopTag Peroxidase In Situ Apoptosis Detection Kit (Chemicon, Temecula, CA, USA), as described previously [20]. Each slide was treated with proteinase K (20 mg/L) for 15 min at room temperature, later 3% hydrogen peroxide to quench endogenous peroxidases for 5 min, and finally incubated with TUNEL reaction mixture containing terminal deoxynucleotidyl transferase (TdT) and digoxigenin-11-dUTP at 37 °C for 1 h. Then 3,3′-diaminobenzidine chromogen was applied, with methyl green as counterstaining. Mouse testicular tissues were used as positive control [29]. For negative control, TdT was omitted from the reaction mixture. Apoptotic cell death was quantitatively

analyzed by counting TUNEL-positive cells randomly from 10 fields, at 400× magnification. Results were presented as the number of TUNEL-positive cells per 10^3 cells.

2.8. Quantitative analysis of lipid peroxides

The lipid peroxide concentration was measured by thiobarbituric acid (TBA) reactivity, that is, the amount of malondialdehyde (MDA) formed during acid hydrolysis of the lipid peroxide compound. The reaction mixtures contained 50 μL protein samples, 20 μL 8.1% sodium dodecyl sulfate (SDS), 150 μL 20% acetic acid solution (pH 3.5), and 210 μL 0.571% TBA. Each sample was prepared in duplicate. The mixtures were incubated at 90 °C for 1 h and cooled on ice. Later, 100 μL distilled water was added, and the mixtures were centrifuged at 4000 rpm for 15 min. After centrifugation, 150 μL from the supernatant of each sample was extracted for measuring absorbance at 540 nm. MDA level was expressed as nmol MDA per milligram tissues.

2.9. Plasma FGF21 assay

Whole blood was collected in a lithium heparin tube (BD, Franklin Lakes, NJ, USA), and centrifuged at 2000 rpm for 20 min at 4 °C. Later, 70 μL of plasma from FGF21-null and WT groups were collected for FGF21 assay using a FGF21 Quantikine Elisa kit (R&D systems, Minneapolis, MN, USA) according to the manufacturer's instructions.

2.10. Statistical analysis

Data were presented as mean±S.D. ($n \geq 5$). Calculation of required animal number in each group was done by statistical power inference used in previous studies [20–22]. Comparisons were performed by one-way ANOVA between different groups. We conducted post hoc pairwise repetitive comparisons using Tukey's test (Origin 8.0 laboratory data analysis and graphing software, OriginLab Corp. Northampton, MA). Statistical significance was considered as $p<0.05$.

3. Results

3.1. Effects of FF on body weight and serum biochemistry profiles in diabetic and control mice

FF treatment did not influence body weight, blood glucose, plasma triglyceride, or cholesterol in non-diabetic mice at either 3 M or 6 M. Among diabetic mice, FF treatment did not alter blood glucose levels, but resulted in significantly higher body weight, lower plasma triglyceride, and lower cholesterol levels at 3 M and 6 M (Table 1).

3.2. FF prevented diabetes-induced renal dysfunction and pathological changes

Renal function was examined by UACR. Diabetes significantly increased UACR from 3 M to 6 M. However, FF treatment significantly reduced UACR among diabetic mice at both 3 M and 6 M (Fig. 1A). Ratios of kidney weight-to-tibia length, an index of renal hypertrophy, significantly increased in DM group compared to Ctrl (Fig. 1B), and were similarly attenuated by FF treatment at both 3 M and 6 M. H&E staining (Fig. 1C) revealed prominent renal structural changes in DM group, including glomerular enlargement, glomerular

basement membrane thickening, mesangial proliferation, and increased mesangial matrix deposition at both 3 M and 6 M. FF treatment significantly ameliorated these pathological alterations. Renal glycogen accumulation by PAS staining increased in a time-dependent manner from 3 M to 6 M in DM group, but not in DM/FF group (Fig. 1D). Significant differences were found in glomerular area and renal glycogen accumulation between DM and DM/FF groups (Fig. 1E and F).

3.3. FF prevented diabetes-induced renal fibrosis, oxidative stress, inflammation, and apoptosis

The fibrotic effect of diabetes on the kidneys, using Western blots, appeared to be lessened from 3 M to 6 M in DM/FF group (Fig. 2A). Diabetes-induced renal fibrosis was also examined by Sirius-red (Fig. 2B and D) and Masson's staining (Fig. 2C and E). Both stains indicated reduced fibrosis in diabetic mice receiving FF.

We further examined the effect of FF on diabetes-induced renal oxidative stress. Western blotting of renal oxidative products showed significantly higher levels of 3-NT (an index of nitrosative damages) and 4-HNE (an index of lipid peroxidation) in DM group compared to Ctrl. However, both 3-NT and 4-HNE accumulation significantly lowered at 3 M and 6 M in DM/FF group compared to DM group (Fig. 3A). MDA showed the same changes as those of 3-NT and 4-HNE in diabetic mice with or without receiving FF (Fig. 3B) [30].

Inflammatory cytokines are also important mediators of diabetes-induced renal damages. Our results showed that renal expressions of inflammatory cytokines, including TNF-α and PAI-1, significantly increased in DM group. However, FF treatment abolished the diabetes-induced cytokine expressions at 3 M and 6 M (Fig. 3C).

Renal cell apoptosis has been reported to be involved in the development of DN. Apoptotic cells were found to increase significantly in the kidneys of DM group, but not in those of DM/FF group compared to Ctrl (Fig. 3D and E). Western blotting revealed significantly higher ratios of Bax to Bcl2 and higher expressions of cleaved caspase-3 (c-Cas-3) in DM group, but not those in DM/FF group (Fig. 3F). These findings confirmed that FF treatment prevented renal cells from apoptosis induced by diabetes.

3.4. FF up-regulated Nrf2 function in the kidneys of diabetic mice

Altering Nrf2 has been reported as a potent anti-oxidative mechanism for preventing DN [2,4]. Immunofluorescent staining showed that the expressions of Nrf2 in the kidneys of DM group increased at 3 M, but decreased at 6 M. FF induced a nuclear accumulation of Nrf2, or its activation, in both non-diabetic and diabetic groups (Fig. 4A). Western blotting further showed that Nrf2 nuclear expressions in kidneys slightly increased at 3 M and decreased at 6 M in diabetic mice, and that FF significantly increased Nrf2 nuclear expressions in kidneys of both normal and diabetic mice, compared to Ctrl without FF treatment (Fig. 4B). These findings were similar to those from immunofluorescent staining.

The function of Nrf2 was further investigated by detecting the expressions of its downstream antioxidant genes, including HO-1 and NQO1. As shown in Fig. 4C and D, the mRNA levels of HO-1 and NQO1 in kidneys significantly increased after FF treatment, consistent

with increased Nrf2 nuclear expressions. These results strongly suggested that FF up-regulated renal Nrf2 function, and this potentially protected kidney from diabetes-induced damages.

3.5. FF increased renal FGF21 expressions and activated the PI3K/Akt/GSK-3β/Fyn pathway

We next examined the expression of FGF21, the target of PPARα that regulates the expressions of Nrf2 [17,31]. Renal FGF21 mRNA expressions significantly decreased in DM group at 3 M and 6 M, but increased in both FF and DM/FF groups. This was also confirmed by Western blotting, which showed the same changing pattern of FGF21 expressions (Fig. 5A and B).

Reports indicated that FGF21 could ameliorate organ damages via activation of the PI3K/Akt pathway in diabetes [17,32,33]. Moreover, the Akt/GSK-3β/Fyn pathway is an important effector of Nrf2 after its activation [34,35]. Diabetic mice without FF treatment showed significantly decreased PI3K and Akt phosphorylation while increased GSK-3β activation, as shown by the decreased *p*-GSK-3β expressions. These findings were accompanied by an increased nuclear accumulation of Fyn in the kidneys (Fig. 5C–E). Compared to DM group, DM/FF group demonstrated preserved PI3K and Akt activation status, but GSK-3β activation was inhibited and nuclear translocation of Fyn was lower in kidney tissues (Fig. 5C–E). These results indicated that FGF21 and PI3K/Akt/GSK-3β/Fyn pathway might be involved in FF-induced up-regulation of Nrf2 function.

3.6. Effects of FF on body weight and serum biochemical profiles in diabetic FGF21-null and WT mice

Diabetes was induced in FGF21-null and WT (C57BL/6J) mice as described above. Diabetes significantly decreased body weight gain in both diabetic WT mice and diabetic FGF21-null mice, with more severe body weight loss in the latter. The diabetes-induced decrease in body weight was prevented by FF in WT mice, but not in FGF21-null mice. FF treatment did not significantly alter blood glucose levels in either diabetic WT or FGF21-null mice. FF treatment did not affect plasma triglyceride or cholesterol levels in either WT or FGF21-null non-diabetic mice, while significantly attenuated both plasma triglyceride and cholesterol levels in diabetic groups. These results suggested that FF-mediated alteration of lipid profiles is FGF21-independent (Table 2).

3.7. Protective effects of FF against diabetes-induced renal damages depend on FGF21

There was no difference in UACR levels between non-diabetic FGF21-null and non-diabetic WT mice (Fig. 6A). UACR levels of diabetic WT mice were higher than those of WT Ctrl mice, but lower than those of diabetic FGF21-null ones, suggesting a protective role of endogenous FGF21 in the process of diabetic kidney damages. More importantly, FF attenuated diabetes-induced increase of UACR levels in WT mice but not in FGF21-null ones.

The increased ratios of kidney weight to tibia length increased significantly in both WT DM and FGF21-null DM group, compared to non-diabetic controls (Fig. 6B). FF attenuated

diabetes-induced increases in kidney weight/tibia length ratio in WT mice but not in FGF21-null ones. Pathological changes and the severity of glycogen accumulation in the kidneys of diabetic FGF21-null mice were worse than those of diabetic WT ones. Compared to WT DM/FF group, the protective effects of FF on these abnormalities were abolished in FGF21-null DM/FF group (Fig. 6C and D). H&E and PAS staining confirmed the pathological changes as well (Fig. 6E and F).

Diabetes significantly induced renal apoptosis (Fig. 7A–C), oxidative damages (Fig. 7D), inflammatory responses (Fig. 7D), and fibrotic effects (Fig. 8) in both WT and FGF21-null mice. These changes were worse in diabetic FGF21-null mice than those in diabetic WT ones, and were significantly reduced in diabetic WT mice receiving FF, but not in diabetic FGF21-null ones receiving FF (Figs. 7 and 8). These results indicated that the effect of FF on diabetes-induced renal damages was FGF21-dependent.

3.8. FGF21 gene deletion abolished FF-induced activation of the PI3K/Akt/GSK-3β/Fyn pathway and Nrf2 function

Compared to normal WT mice, the levels of plasma FGF21 (Fig. 9A) and renal FGF21 mRNA (Fig. 9B) increased in FF-treated WT ones, but decreased in diabetic WT ones. These levels remained unchanged in FF-treated diabetic WT mice. Plasma FGF21 protein and renal FGF21 mRNA were undetectable in FGF21-null mice with or without FF administration.

Western blotting showed that, compared to non-diabetic WT mice without receiving FF (Ctrl), the ratios of *p*-PI3K to *t*-PI3K, *p*-Akt to *t*-Akt, and also *p*-GSK-3β to *t*-GSK-3β significantly increased in FF-treated WT mice, but significantly decreased in diabetic mice without receiving FF. However, the ratios remained unchanged in diabetic WT mice receiving FF (Fig. 9C–E), but the levels decreased in diabetic FGF21-null mice compared to diabetic WT ones. The effects of FF on either non-diabetic or diabetic FGF21-null mice were not statistically significant (Fig. 9C–E).

In WT mice, FF attenuated diabetes-induced nuclear accumulation of Fyn (Fig. 9F). In diabetic FGF21-null mice, diabetes increased more prominent nuclear accumulation of Fyn than that in diabetic WT ones. However, FF did not restore diabetes-increased nuclear accumulation of Fyn in diabetic FGF21-null mice (Fig. 9F).

FF treatment increased the nuclear accumulation of Nrf2 in WT mice with or without diabetes (Fig. 9G). FF failed to stimulate the nuclear accumulation of Nrf2 in diabetic FGF21-null mice, although these mice showed more significant decreases in nuclear accumulation of Nrf2 than diabetic WT ones (Fig. 9G). The expression of NQO1 exhibited similar pattern as Nrf2 (Fig. 9H). These findings collectively indicated that FF can ameliorate diabetes-induced renal damages, and these effects are mediated by FGF21. Deletion of the FGF21 gene abolishes the FF-induced activation of the PI3K/Akt/GSK-3β/Fyn pathway and Nrf2 functions.

4. Discussion

Although FF is used clinically for type 2 diabetic patients [9,10], its application in type 1 diabetic patients has not been well explored [13–15]. Using a STZ-induced diabetic mouse model, we demonstrated that FF significantly ameliorates DN. We reported for the first time that type 1 diabetes is associated with down-regulation of renal FGF21 expressions at both mRNA and protein levels. FF significantly increased renal FGF21 expressions in both non-diabetic and diabetic mice. Using FGF21-null mice, we demonstrated that the effect of FF on diabetic renal damages is FGF21-dependent. We further identified that this FGF21-mediated renal effects is associated with the activation of Nrf2. The Nrf2 activation is further mediated by a FGF21-dependent PI3K/Akt/GSK-3β/Fyn pathway, as summarized in Fig. 10.

Few studies have explored the preventive effect of FF against STZ-induced diabetic damages to the kidneys [13–15]. Among these studies, most reported that FF protects the kidney from diabetes beyond its lipid-lowering action. Others found that the renal protection offered by FF in diabetes might be dependent on PPARα, evidenced by the accelerated development of DN in mice with PPARα deficiency [36]. Studies finding that FF treatment reduced DOX-induced renal damages only in PPARα normal mice, but not in PPARα deficient ones also indirectly support the above notions [11,12]. Although the above studies affirm the preventive effect of FF against both type 1 and type 2 diabetes-induced renal damages, it remains unclear how FF protects the kidneys in type 1 diabetic patients beyond its lipid-lowering effect [10]. Our findings expand the existing evidence by demonstrating the pivotal role of FGF21 in FF-mediated renal protection from diabetes.

As a downstream effector of PPARα, FGF21 possesses hypoglycemic, lipid-lowering, and thermogenic properties [31]. Induction of blood FGF21 levels in humans by FF treatment has been described previously [37,38]. Evidence suggests that renal expressions of FGF21 did not change at 2 months, but significant decreased at 5 months after diabetes development in a db/db type 2 diabetes model [39]. Consistent with their findings, we also found that renal FGF21 expressions gradually decreased from 3 to 6 months (Fig. 5A and B), although the levels increased at 1 month after diabetes (data not shown). Another in vitro study showed that mesangial cells had increased FGF21 mRNA and protein expressions in response to TGF-β1 in a time-dependent manner (6–9 h at peak but diminished at 24 h [40]). Adding up our results, studies suggest that FGF21 is up-regulated in the early stage of diabetes to protect the kidney from pathogenic changes induced by diabetes or TGF-β1. During decompensation, FGF21 may decrease at late stages of diabetes with the concomitant renal damages. Information that extrapolates from studies on other organs may support this concept. First, oxidative stress, lipotoxicity, and endoplasmic reticulum (ER) stress can increase cardiac FGF21 expressions [19,41]. Second, exogenous supplement of FGF21 or cardiac overexpression of FGF21 have been shown to exert cardiac protection against various challenges [19,42,43]. Past studies reported that supplementation of exogenous FGF21 could protect the kidney from type 1 and type 2 diabetes-induced pathological changes [39,44]. We further provided direct evidence in this study that diabetic FGF21-null mice exhibited severe renal pathological and functional abnormalities (Figs. 6–8).

A novel finding of this study is that we discover a potential mechanism by which FGF21 protects against DN, the up-regulation of Nrf2 function. Nrf2 orchestrates multiple antioxidants for protecting against the oxidative damage associated with DN [2,5,6]. Zhang et al. used Nrf2 activators (sulforaphane or cinnamic aldehyde) to treat STZ-induce diabetic model in both Nrf2-null and WT mice [5]. They demonstrated that the activation of Nrf2 and its targets NQO1 and γ-glutamylcysteine synthetase (γ-GCS) significantly prevents the development of DN in STZ-induced diabetic WT mice, but not in diabetic Nrf2-null ones [5]. More importantly, Bardoxolone methyl (also known as CDDO-Me or RTA 402), via induction of Nrf2, has been extensively explored for its preventive and therapeutic effects against DN [45,46], although it was withdrawn due to toxic effects [47]. These results suggests that although activation of Nrf2 is a promising target to prevent DN, the potentially associated toxic effects are significant concern when developing activators of Nrf2. If FF can act as a Nrf2 activator via the FGF21-dependent mechanism, it may possess therapeutic promise, since FF has been used widely in clinical practice, and is safe and well tolerated.

Another important finding in this study is the potential insight into how FGF21 mediates Nrf2 activation to protect the kidneys from diabetes. Existing evidence regarding the cross-talk between Nrf2 and FGF21 is scanty. One study suggests an inhibitory effect of Nrf2 on FGF21 induction [48]; another study reported a positive regulation of FGF21 by Nrf2 [49], while other studies identified Nrf2 induction by FGF21 [16,17]. These findings suggest a complex association between FGF21 and Nrf2. In this study, we found that FF-induced Nrf2 was dependent on FGF21 (Fig. 9G and H). The mechanism through which FGF21 activates remains largely unknown. We further provided in vivo evidence for the first time that FGF21 may activate the Nrf2 expression in the nuclei by activation of PI3K/Akt/GSK-3β-dependent inhibition of Fyn nuclear translocation. In WT mice, FF-induced FGF21 expression was associated with increased PI3K, Akt, and GSK-3β phosphorylation as well as decreased Fyn nuclear accumulation. In FGF21-null mice, FF failed to increase PI3K, Akt, and GSK-3β phosphorylation but subsequently decreased Fyn nuclear accumulation (Fig. 9C–F). It has been known that Fyn translocates into nuclei and exports nuclear Nrf2 to cytosol, where it binds to Keap1 for degradation [50,51]. Therefore, we assume that Nrf2 activation by FF in WT mice may be mediated by the FGF21-mediated increase in PI3K, Akt, and GSK-3β phosphorylation, and the subsequent decrease in Fyn nuclear accumulation. This could restore Nrf2 nuclear localization and have Nrf2 exert its action, as illustrated in Fig. 10.

There are a few limitations in the present study. First, the evidence for the possible mechanism we provided is indirect in nature (Fig. 10); the mechanistic pathway needs to be further defined in future studies. Second, although we discover the potential use of FF for the treatment DN and investigate the mechanisms through which FF may prevent DN, further investigation is needed using other diabetes models (for instance, OVE26 mice); clinical trials are also needed to further confirm the protective role of FF in DN. Further confirmatory studies concerning the mechanisms, animal models, and clinic trials can provide the theoretical base for the clinical application of FF.

Acknowledgments

This work was supported in part by grants from the National Natural Science Foundation of China (81300660 to W.G.; 81202151 to F.L.; 81400725 to W.S.; 81471045 to X.L.; 81270809 to Z.X.), the Graduate Innovation Fund of Jilin University (2015032 to Y.C.), the Juvenile Diabetes Research Foundation (1-INO-2014-122-A-N to Y. T.), and the National Institutes of Health (1R01DK091338-01A1 to L.C.).

References

[1]. Keshari KR, Wilson DM, Sai V, Bok R, Jen KY, Larson P, Van Criekinge M, Kurhanewicz J, Wang ZJ, Noninvasive in vivo imaging of diabetes-induced renal oxidative stress and response to therapy using hyperpolarized 13C dehydroascorbate magnetic resonance, Diabetes 64 (2015) 344–352. [PubMed: 25187363]

[2]. Li B, Liu S, Miao L, Cai L, Prevention of diabetic complications by activation of Nrf2: diabetic cardiomyopathy and nephropathy, Exp. Diabetes Res 2012 (2012) 216512. [PubMed: 22645602]

[3]. Miyata T, Suzuki N, van Ypersele de Strihou C, Diabetic nephropathy: are there new and potentially promising therapies targeting oxygen biology? Kidney Int 84 (2013) 693–702. [PubMed: 23486514]

[4]. de Haan JB, Nrf2 activators as attractive therapeutics for diabetic nephropathy, Diabetes 60 (2011) 2683–2684. [PubMed: 22025774]

[5]. Zheng H, Whitman SA, Wu W, Wondrak GT, Wong PK, Fang D, Zhang DD, Therapeutic potential of Nrf2 activators in streptozotocin-induced diabetic nephropathy, Diabetes 60 (2011) 3055–3066. [PubMed: 22025779]

[6]. Jiang T, Huang Z, Lin Y, Zhang Z, Fang D, Zhang DD, The protective role of Nrf2 in streptozotocin-induced diabetic nephropathy, Diabetes 59 (2010) 850–860. [PubMed: 20103708]

[7]. Strittmatter SM, Overcoming drug development bottlenecks with repurposing: old drugs learn new tricks, Nat. Med 20 (2014) 590–591. [PubMed: 24901567]

[8]. Higgins MJ, Thursby J, Thursby M, Bench-to-bench bottlenecks in translation, Sci. Transl. Med 6 (2014) 250fs232.

[9]. Ansquer JC, Foucher C, Rattier S, Taskinen MR, Steiner G, D. Investigators, Fenofibrate reduces progression to microalbuminuria over 3 years in a placebo-controlled study in type 2 diabetes: results from the Diabetes Atherosclerosis Intervention Study (DAIS), Am. J. Kidney Dis 45 (2005) 485–493. [PubMed: 15754270]

[10]. Hong YA, Lim JH, Kim MY, Kim TW, Kim Y, Yang KS, Park HS, Choi SR, Chung S, Kim HW, Kim HW, Choi BS, Chang YS, Park CW, Fenofibrate improves renal lipotoxicity through activation of AMPK-PGC-1alpha in db/db mice, PLoS One 9 (2014) e96147. [PubMed: 24801481]

[11]. Zhou Y, Kong X, Zhao P, Yang H, Chen L, Miao J, Zhang X, Yang J, Ding J, Guan Y, Peroxisome proliferator-activated receptor-alpha is renoprotective in doxorubicin-induced glomerular injury, Kidney Int 79 (2011) 1302–1311. [PubMed: 21368746]

[12]. Mori K, Mukoyama M, Nakao K, PPAR-alpha transcriptional activity is required to combat doxorubicin-induced podocyte injury in mice, Kidney Int 79 (2011) 1274–1276. [PubMed: 21625258]

[13]. Chen LL, Zhang JY, Wang BP, Renoprotective effects of fenofibrate in diabetic rats are achieved by suppressing kidney plasminogen activator inhibitor-1, Vascul. Pharmacol 44 (2006) 309–315. [PubMed: 16624630]

[14]. Chen L, Zhang J, Zhang Y, Wang Y, Wang B, Improvement of inflammatory responses associated with NF-kappa B pathway in kidneys from diabetic rats, Inflamm. Res 57 (2008) 199–204. [PubMed: 18465086]

[15]. Kadian S, Mahadevan N, Balakumar P, Differential effects of low-dose fenofibrate treatment in diabetic rats with early onset nephropathy and established nephropathy, Eur. J. Pharmacol 698 (2013) 388–396. [PubMed: 23085026]

[16]. Ye D, Wang Y, Li H, Jia W, Man K, Lo CM, Wang Y, Lam KS, Xu A, Fibroblast growth factor 21 protects against acetaminophen-induced hepatotoxicity by potentiating peroxisome proliferator-

activated receptor coactivator protein-1alpha-mediated antioxidant capacity in mice, Hepatology 60 (2014) 977–989. [PubMed: 24590984]

[17]. Yu Y, Bai F, Liu Y, Yang Y, Yuan Q, Zou D, Qu S, Tian G, Song L, Zhang T, Li S, Liu Y, Wang W, Ren G, Li D, Fibroblast growth factor (FGF21) protects mouse liver against D-galactose-induced oxidative stress and apoptosis via activating Nrf2 and PI3K/Akt pathways, Mol. Cell. Biochem 403 (2015) 287–299. [PubMed: 25701356]

[18]. Jiang X, Zhang C, Xin Y, Huang Z, Tan Y, Huang Y, Wang Y, Feng W, Li X, Li W, Qu Y, Cai L, Protective effect of FGF21 on type 1 diabetes-induced testicular apoptotic cell death probably via both mitochondrial- and endoplasmic reticulum stress-dependent pathways in the mouse model, Toxicol. Lett 219 (2013) 65–76. [PubMed: 23499715]

[19]. Planavila A, Redondo-Angulo I, Ribas F, Garrabou G, Casademont J, Giralt M, Villarroya F, Fibroblast growth factor 21 protects the heart from oxidative stress, Cardiovasc. Res 106 (2015) 19–31. [PubMed: 25538153]

[20]. Cai L, Li W, Wang G, Guo L, Jiang Y, Kang YJ, Hyperglycemia-induced apoptosis in mouse myocardium: mitochondrial cytochrome C-mediated caspase-3 activation pathway, Diabetes 51 (2002) 1938–1948. [PubMed: 12031984]

[21]. Cai L, Wang J, Li Y, Sun X, Wang L, Zhou Z, Kang YJ, Inhibition of superoxide generation and associated nitrosative damage is involved in metallothionein prevention of diabetic cardiomyopathy, Diabetes 54 (2005) 1829–1837. [PubMed: 15919806]

[22]. Wang Y, Wang Y, Luo M, Wu H, Kong L, Xin Y, Cui W, Zhao Y, Wang J, Liang G, Miao L, Cai L, Novel curcumin analog C66 prevents diabetic nephropathy via JNK pathway with the involvement of p300/CBP-mediated histone acetylation, Biochim. Biophys. Acta 2015 (1852) 34–46.

[23]. Whelton BD, Peterson DP, Moretti ES, Mauser RW, Bhattacharyya MH, Kidney changes in multiparous, nulliparous and ovariectomized mice fed either a nutrient-sufficient or -deficient diet containing cadmium, Toxicology 119 (1997) 123–140. [PubMed: 9128185]

[24]. Jeansson M, Granqvist AB, Nystrom JS, Haraldsson B, Functional and molecular alterations of the glomerular barrier in long-term diabetes in mice, Diabetologia 49 (2006) 2200–2209. [PubMed: 16868749]

[25]. Cui W, Bai Y, Miao X, Luo P, Chen Q, Tan Y, Rane MJ, Miao L, Cai L, Prevention of diabetic nephropathy by sulforaphane: possible role of nrf2 upregulation and activation, Oxid. Med. Cell Longev 2012 (2012) 821936. [PubMed: 23050040]

[26]. Cai L, Wang Y, Zhou G, Chen T, Song Y, Li X, Kang YJ, Attenuation by metallothionein of early cardiac cell death via suppression of mitochondrial oxidative stress results in a prevention of diabetic cardiomyopathy, J. Am. Coll. Cardiol 48 (2006) 1688–1697. [PubMed: 17045908]

[27]. Sun W, Wang Y, Miao X, Wang Y, Zhang L, Xin Y, Zheng S, Epstein PN, Fu Y, Cai L, Renal improvement by zinc in diabetic mice is associated with glucose metabolism signaling mediated by metallothionein and Akt, but not Akt2, Free Radic. Biol. Med 68 (2014) 22–34. [PubMed: 24296248]

[28]. Cui W, Li B, Bai Y, Miao X, Chen Q, Sun W, Tan Y, Luo P, Zhang C, Zheng S, Epstein PN, Miao L, Cai L, Potential role for Nrf2 activation in the therapeutic effect of MG132 on diabetic nephropathy in OVE26 diabetic mice, Am. J. Physiol. Endocrinol. Metab 304 (2013) E87–E99. [PubMed: 23132297]

[29]. Cai L, Chen S, Evans T, Deng DX, Mukherjee K, Chakrabarti S, Apoptotic germ-cell death and testicular damage in experimental diabetes: prevention by endothelin antagonism, Urol. Res 28 (2000) 342–347. [PubMed: 11127715]

[30]. Baynes JW, Thorpe SR, Role of oxidative stress in diabetic complications: a new perspective on an old paradigm, Diabetes 48 (1999) 1–9. [PubMed: 9892215]

[31]. Badman MK, Pissios P, Kennedy AR, Koukos G, Flier JS, Maratos-Flier E, Hepatic fibroblast growth factor 21 is regulated by PPARalpha and is a key mediator of hepatic lipid metabolism in ketotic states, Cell Metab 5 (2007) 426–437. [PubMed: 17550778]

[32]. Wente W, Efanov AM, Brenner M, Kharitonenkov A, Koster A, Sandusky GE, Sewing S, Treinies I, Zitzer H, Gromada J, Fibroblast growth factor-21 improves pancreatic beta-cell

function and survival by activation of extracellular signal-regulated kinase 1/2 and Akt signaling pathways, Diabetes 55 (2006) 2470–2478. [PubMed: 16936195]

[33]. Jiang X, Chen J, Zhang C, Zhang Z, Tan Y, Feng W, Skibba M, Xin Y, Cai L, The protective effect of FGF21 on diabetes-induced male germ cell apoptosis is associated with up-regulated testicular AKT and AMPK/Sirt1/PGC-1alpha signaling, Endocrinology 156 (2015) 1156–1170. [PubMed: 25560828]

[34]. Rizvi F, Shukla S, Kakkar P, Essential role of PH domain and leucine-rich repeat protein phosphatase 2 in Nrf2 suppression via modulation of Akt/GSK3beta/Fyn kinase axis during oxidative hepatocellular toxicity, Cell Death Dis 5 (2014) e1153. [PubMed: 24675471]

[35]. Li B, Cui W, Tan Y, Luo P, Chen Q, Zhang C, Qu W, Miao L, Cai L, Zinc is essential for the transcription function of Nrf2 in human renal tubule cells in vitro and mouse kidney in vivo under the diabetic condition, J. Cell. Mol. Med 18 (2014) 895–906. [PubMed: 24597671]

[36]. Park CW, Kim HW, Ko SH, Chung HW, Lim SW, Yang CW, Chang YS, Sugawara A, Guan Y, Breyer MD, Accelerated diabetic nephropathy in mice lacking the peroxisome proliferator-activated receptor alpha, Diabetes 55 (2006) 885–893. [PubMed: 16567507]

[37]. Galman C, Lundasen T, Kharitonenkov A, Bina HA, Eriksson M, Hafstrom I, Dahlin M, Amark P, Angelin B, Rudling M, The circulating metabolic regulator FGF21 is induced by prolonged fasting and PPARalpha activation in man, Cell Metab 8 (2008) 169–174. [PubMed: 18680716]

[38]. Ong KL, Rye KA, O'Connell R, Jenkins AJ, Brown C, Xu A, Sullivan DR, Barter PJ, Keech AC, Investigators FS, Long-term fenofibrate therapy increases fibroblast growth factor 21 and retinol-binding protein 4 in subjects with type 2 diabetes, J. Clin. Endocrinol. Metab 97 (2012) 4701–4708. [PubMed: 23144467]

[39]. Kim HW, Lee JE, Cha JJ, Hyun YY, Kim JE, Lee MH, Song HK, Nam DH, Han JY, Han SY, Han KH, Kang YS, Cha DR, Fibroblast growth factor 21 improves insulin resistance and ameliorates renal injury in db/db mice, Endocrinology 154 (2013) 3366–3376. [PubMed: 23825123]

[40]. Loeffler I, Hopfer U, Koczan D, Wolf G, Type VIII collagen modulates TGF-beta1-induced proliferation of mesangial cells, J. Am. Soc. Nephrol 22 (2011) 649–663. [PubMed: 21372207]

[41]. Brahma MK, Adam RC, Pollak NM, Jaeger D, Zierler KA, Pocher N, Schreiber R, Romauch M, Moustafa T, Eder S, Ruelicke T, Preiss-Landl K, Lass A, Zechner R, Haemmerle G, Fibroblast growth factor 21 is induced upon cardiac stress and alters cardiac lipid homeostasis, J. Lipid Res 55 (2014) 2229–2241. [PubMed: 25176985]

[42]. Planavila A, Redondo I, Hondares E, Vinciguerra M, Munts C, Iglesias R, Gabrielli LA, Sitges M, Giralt M, van Bilsen M, Villarroya F, Fibroblast growth factor 21 protects against cardiac hypertrophy in mice, Nat. Commun 4 (2013) 2019. [PubMed: 23771152]

[43]. Cong WT, Ling J, Tian HS, Ling R, Wang Y, Huang BB, Zhao T, Duan YM, Jin LT, Li XK, Proteomic study on the protective mechanism of fibroblast growth factor 21 to ischemia–reperfusion injury, Can. J. Physiol. Pharmacol 91 (2013) 973–984. [PubMed: 24117266]

[44]. Zhang C, Shao M, Yang H, Chen L, Yu L, Cong W, Tian H, Zhang F, Cheng P, Jin L, Tan Y, Li X, Cai L, Lu X, Attenuation of hyperlipidemia- and diabetes-induced early-stage apoptosis and late-stage renal dysfunction via administration of fibroblast growth factor-21 is associated with suppression of renal inflammation, PLoS One 8 (2013) e82275. [PubMed: 24349242]

[45]. Pergola PE, Krauth M, Huff JW, Ferguson DA, Ruiz S, Meyer CJ, Warnock DG, Effect of bardoxolone methyl on kidney function in patients with T2D and stage 3b-4 CKD, Am. J. Nephrol 33 (2011) 469–476. [PubMed: 21508635]

[46]. Pergola PE, Raskin P, Toto RD, Meyer CJ, Huff JW, Grossman EB, Krauth M, Ruiz S, Audhya P, Christ-Schmidt H, Wittes J, Warnock DG, Investigators BS, Bardoxolone methyl and kidney function in CKD with type 2 diabetes, N. Engl. J. Med 365 (2011) 327–336. [PubMed: 21699484]

[47]. de Zeeuw D, Akizawa T, Audhya P, Bakris GL, Chin M, Christ-Schmidt H, Goldsberry A, Houser M, Krauth M, Lambers Heerspink HJ, McMurray JJ, Meyer CJ, Parving HH, Remuzzi G, Toto RD, Vaziri ND, Wanner C, Wittes J, Wrolstad D, Chertow GM, Investigators BT, Bardoxolone methyl in type 2 diabetes and stage 4 chronic kidney disease, N. Engl. J. Med 369 (2013) 2492–2503. [PubMed: 24206459]

[48]. Chartoumpekis DV, Ziros PG, Psyrogiannis AI, Papavassiliou AG, Kyriazopoulou VE, Sykiotis GP, Habeos IG, Nrf2 represses FGF21 during long-term high-fat diet-induced obesity in mice, Diabetes 60 (2011) 2465–2473. [PubMed: 21852674]

[49]. Furusawa Y, Uruno A, Yagishita Y, Higashi C, Yamamoto M, Nrf2 induces fibroblast growth factor 21 in diabetic mice, Genes Cells 19 (2014) 864–878. [PubMed: 25270507]

[50]. Koo JH, Lee WH, Lee CG, Kim SG, Fyn inhibition by cycloalkane-fused 1,2-dithiole-3-thiones enhances antioxidant capacity and protects mitochondria from oxidative injury, Mol. Pharmacol 82 (2012) 27–36. [PubMed: 22474169]

[51]. Jain AK, Jaiswal AK, GSK-3beta acts upstream of Fyn kinase in regulation of nuclear export and degradation of NF-E2 related factor 2, J. Biol. Chem 282 (2007) 16502–16510. [PubMed: 17403689]

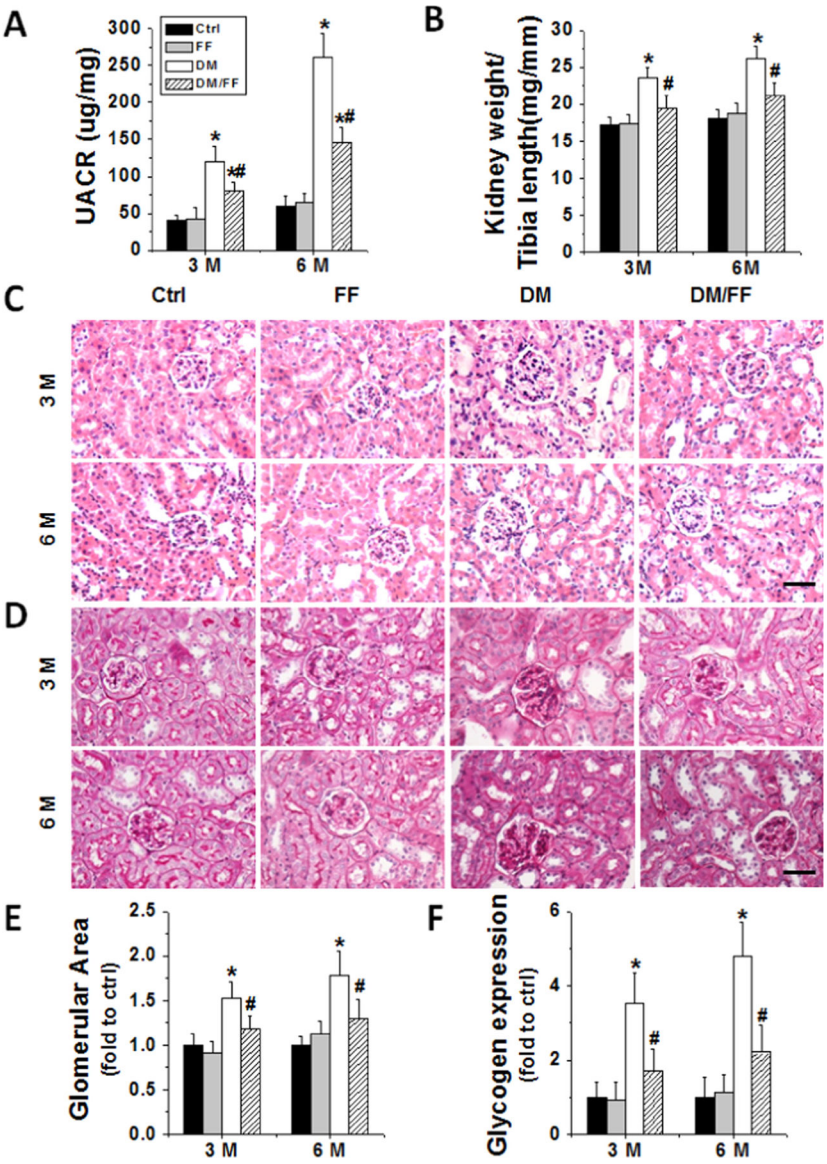

Fig. 1.

FF prevented diabetes-induced renal dysfunction and pathological changes. Diabetes was induced with a single intraperitoneal injection of streptozotocin (STZ, 150 mg/kg), with or without FF (100 mg/kg) every other day for 3 and 6 months. Urinary albumin to creatinine ratio (UACR) (A) and kidney weight to tibia length ratio (B) were measured and calculated at 3 M and 6 M, respectively. Renal morphological changes (C) and glycogen (purple) expressions (D) were examined by hematoxylin and eosin (H&E) and periodic acid-Schiff (PAS) staining in kidney sections (400×, scale bare 100 μm). Glomerular areas (E) and the relative densities of glycogen expressions per image (F) were counted in ten visual fields across the kidneys. Data are presented as the mean±S.D. ($n \geq 5$). * $p<0.05$ vs. corresponding Ctrl; # $p<0.05$ vs. corresponding DM.

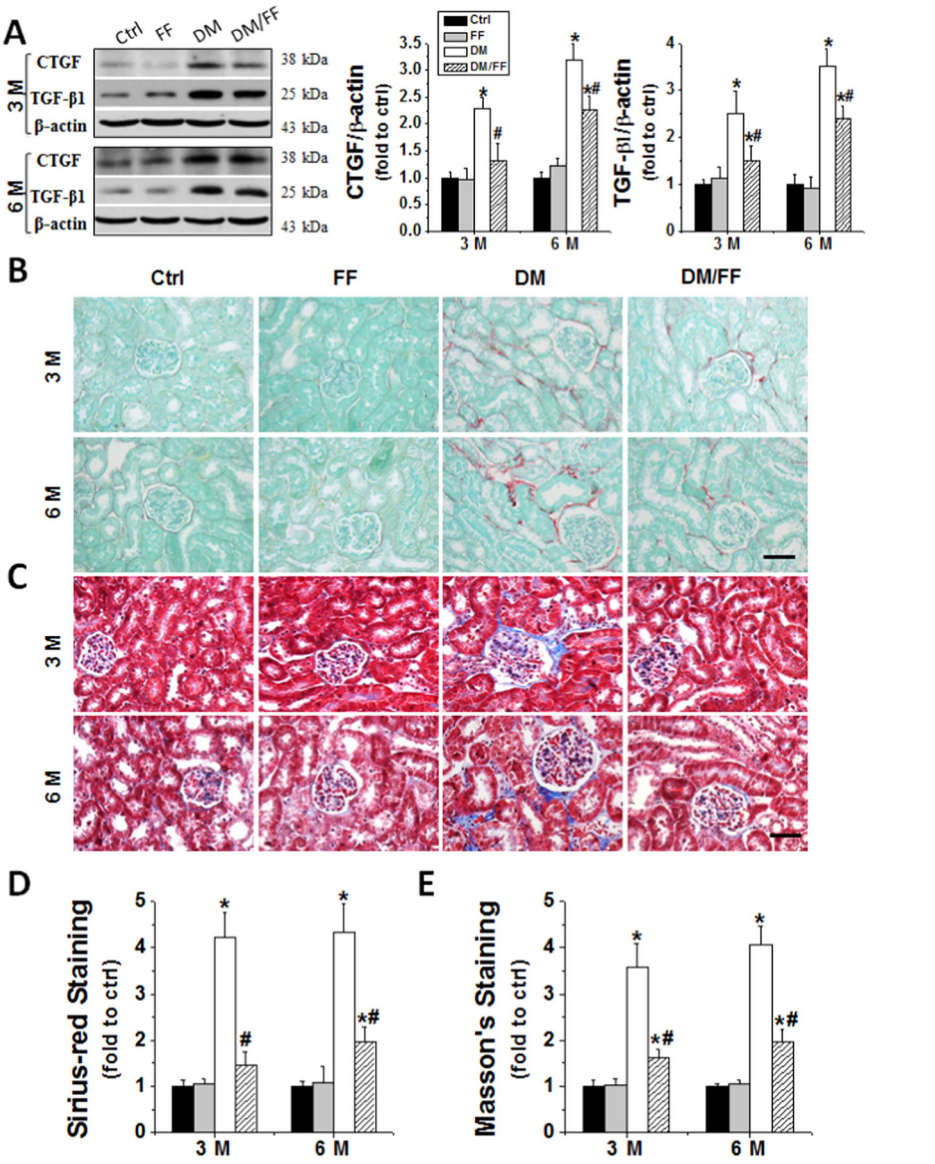

Fig. 2.

FF prevented diabetes-induced renal fibrotic effect. Renal fibrotic response was assessed by an increased expression of connective tissue growth factor (CTGF) and transforming growth factor-β1 (TGF-β1) at 3 M and 6 M, respectively, using Western blotting (A). Sirius-red (B) and Masson's staining (C) were used for detecting collagen fibers (red and blue) in kidney sections (400×, scale bare 100 μm). Semi-quantitative data for Sirius-red and Masson's staining were presented as (D) and (E), respectively. Data are presented as the mean±S.D. ($n \geq 5$). * $p<0.05$ vs. corresponding Ctrl; # $p<0.05$ vs. corresponding DM.

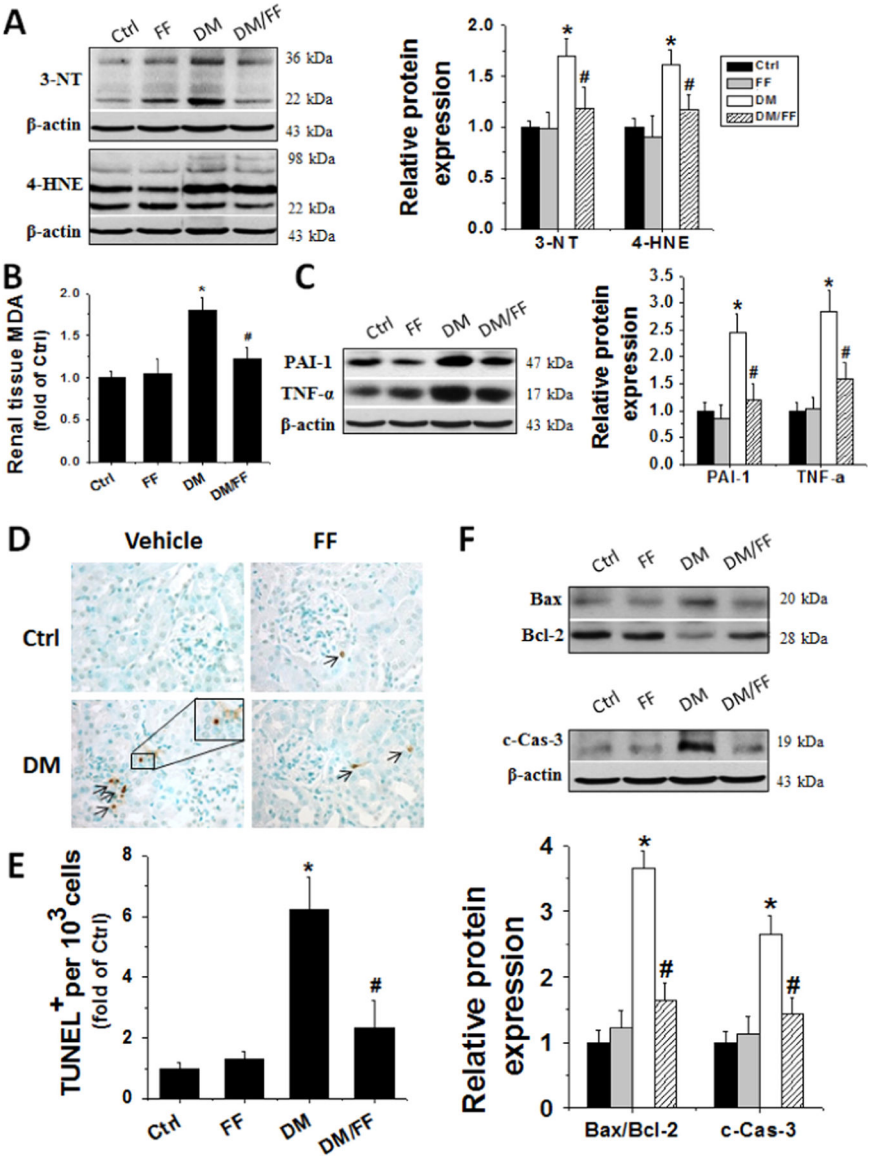

Fig. 3.

FF prevented diabetes-induced renal oxidative damages, inflammation, and apoptosis. Renal tissues were harvested at 3 M. Renal oxidative damages were evaluated by Western blotting for 3-nitrotyrosine (3-NT) and 4-hydroxy-2-nonenal (4-HNE), respectively (A). Lipid peroxidation was measured using malondialdehyde (MDA) content (B). Renal inflammation was detected with plasminogen activator inhibitor-1 (PAI-1) and tumor necrosis factor-α (TNF-α) by Western blotting (C). Renal cell apoptotic death was examined by TUNEL staining (D) (apoptotic cells shown by brown nuclei), followed by quantitative analysis (E) and by Western blotting of Bax to Bcl-2 ratios (Bax/Bcl-2) and cleaved-caspase 3 (c-Cas-3) levels (F). Data are presented as the mean±S.D. ($n \geq 5$). * $p<0.05$ vs. corresponding Ctrl; # $p<0.05$ vs. corresponding DM.

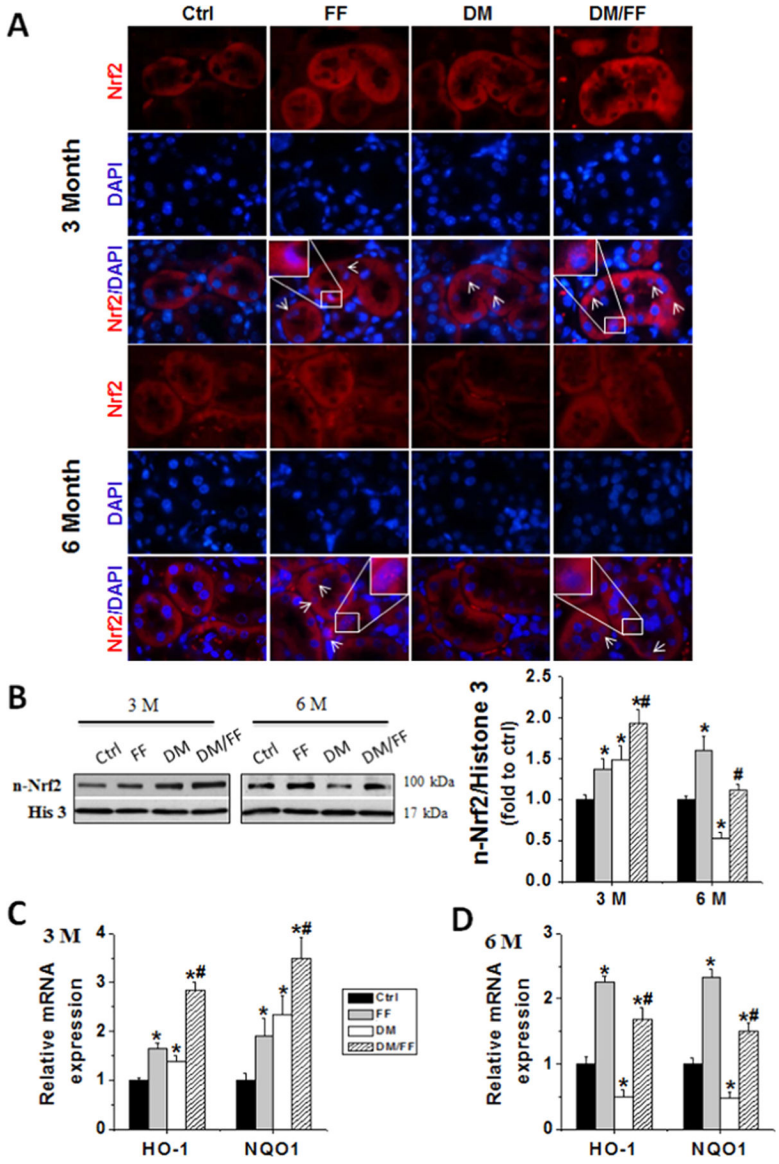

Fig. 4.

FF treatment up-regulated Nrf2 function in the kidney of diabetic mice. The activation of Nrf2 was assessed by its nuclear accumulation (arrowed cells), determined by immunofluorescent staining with Nrf2 antibody (red) and nuclear staining with 4,6-diamidino-2-phenylindole (DAPI, blue) on kidney tissue sections (A) (oil immersion, 1000×). The nuclear expression of Nrf2 was detected by Western blotting at 3 M and 6 M, respectively (B). Nrf2 transcription was assessed by qRT-PCR of Nrf2 downstream genes, including heme oxygenase-1 (HO-1) and NAD(P)H: quinone oxidoreductase 1 (NQO1) at 3 M (C) and 6 M (D), respectively. Data are presented as the mean±S.D. ($n \geq 5$). * $p<0.05$ vs. corresponding Ctrl; # $p<0.05$ vs. corresponding DM.

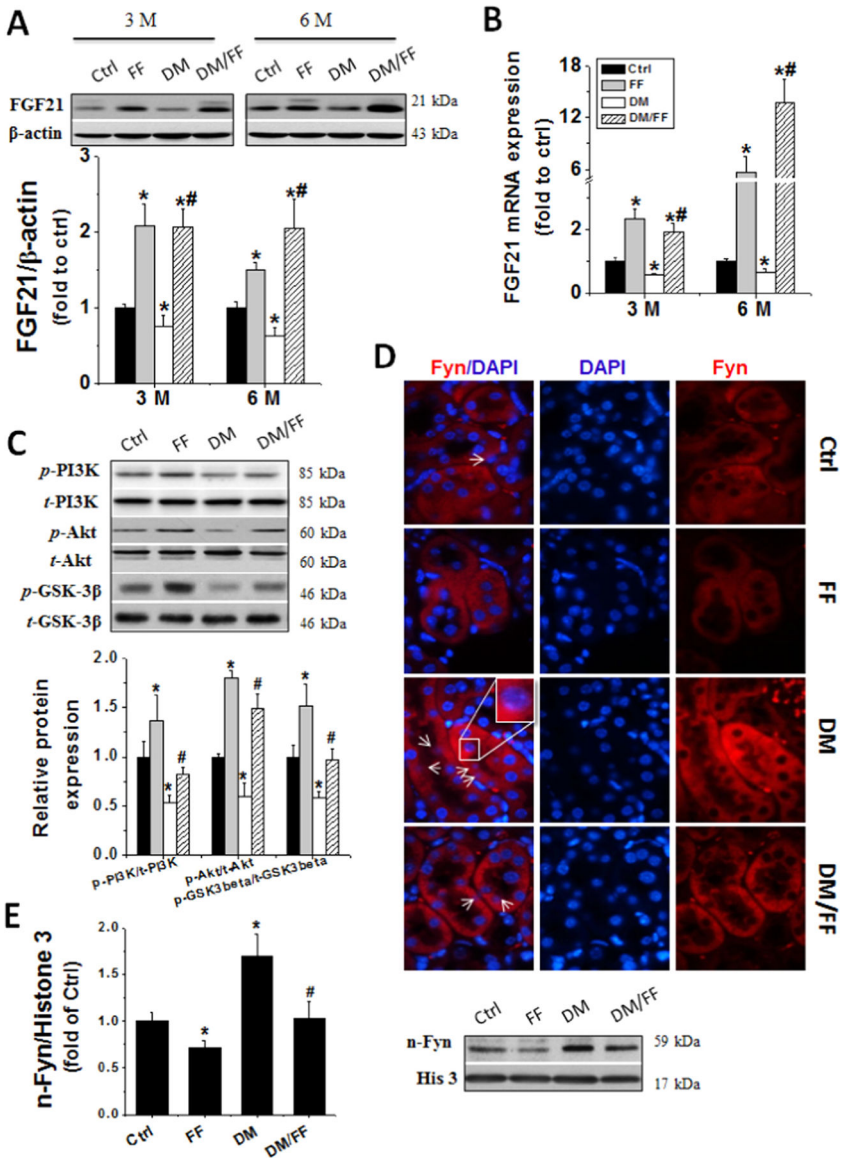

Fig. 5.

FF increased renal FGF21 expression and activated the PI3K/Akt/GSK-3β/Fyn pathway. Renal FGF21 protein expressions were examined with Western blot (A) and relative FGF21 mRNA expressions were assessed by qRT-PCR (B) at 3 M and 6 M, respectively. Renal PI3K and Akt activation as well as GSK-3β inhibition were examined with Western blot (C). The activation of Fyn was assessed by its nuclear accumulation (arrow indicated), using immunofluorescent staining with Fyn antibody (red), nuclear staining with DAPI (blue) on kidney tissue sections (D) (oil immersion, 1000×), and by Western blotting of its expression in nuclear protein (E). Data are presented as the mean±S.D. ($n \geq 5$). * $p<0.05$ vs. corresponding Ctrl; # $p<0.05$ vs. corresponding DM.

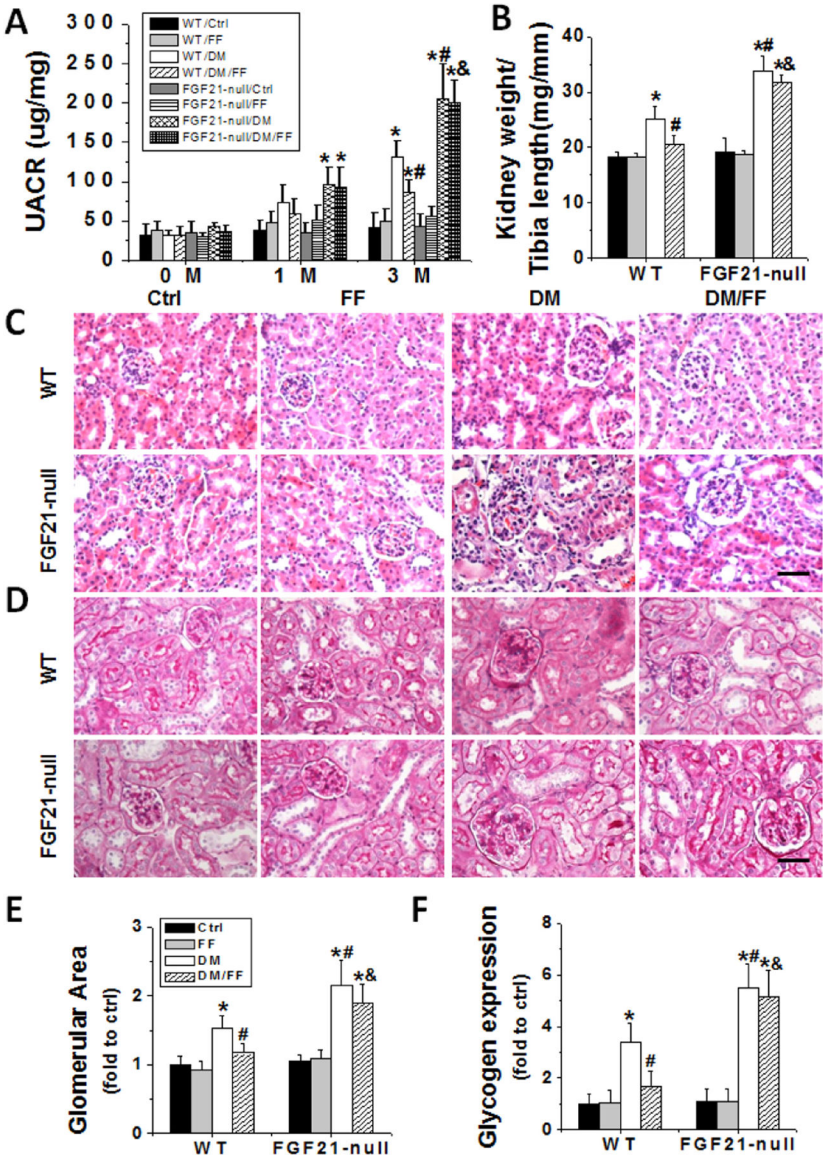

Fig. 6.

FGF21 gene deletion abolished the protective effects of FF against diabetes-induced renal dysfunction and pathological changes. Diabetes was induced in WT and FGF21-null mice with STZ, with or without treatment of FF (100 mg/kg) every other day for 3 months. The UACR (A) was measured before STZ injection (as 0 M), at 1 M and 3 M after diabetes onset. Kidney weight to tibia length ratios (B) were calculated at 3 M. H&E (C) and PAS (D) staining were used to examine renal morphological changes and glycogen (purple) expressions in kidney sections (400×, scale bare 100 μm). Glomerular areas (E) and relative glycogen depositions (F) were estimated. Data are presented as the mean±S.D. ($n \geq 5$). * $p<0.05$ vs. corresponding WT/Ctrl; # $p<0.05$ vs. corresponding WT/DM; & $p<0.05$ vs. corresponding WT/DM/FF.

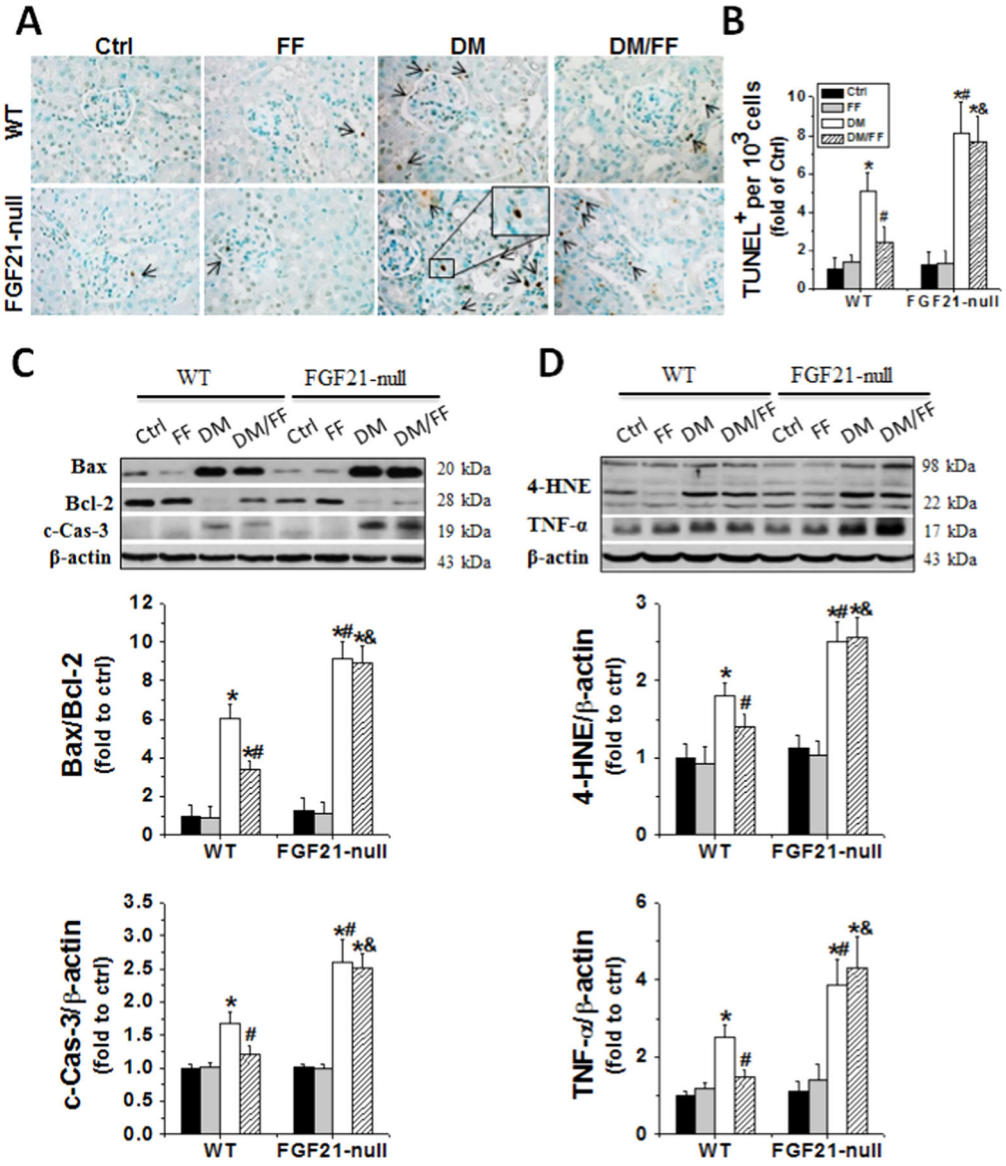

Fig. 7.

FGF21 gene deletion abolished the protective effects of FF against diabetes-induced renal oxidative damage, inflammation, and apoptosis. Renal cell apoptotic death was examined by TUNEL staining (brown) (A), followed by quantitative analysis (B); and by Western blotting for the expression of Bax to Bcl-2 ratios and c-Cas-3 (C) at 3 M. Renal oxidative damages and inflammation statuses were evaluated by Western blotting of 4-HNE and TNF-α expressions at 3 M (D). Data are presented as the mean±S.D. ($n \geq 5$). * $p<0.05$ vs. WT/Ctrl; # $p<0.05$ vs. WT/DM; & $p<0.05$ vs. WT/DM/FF.

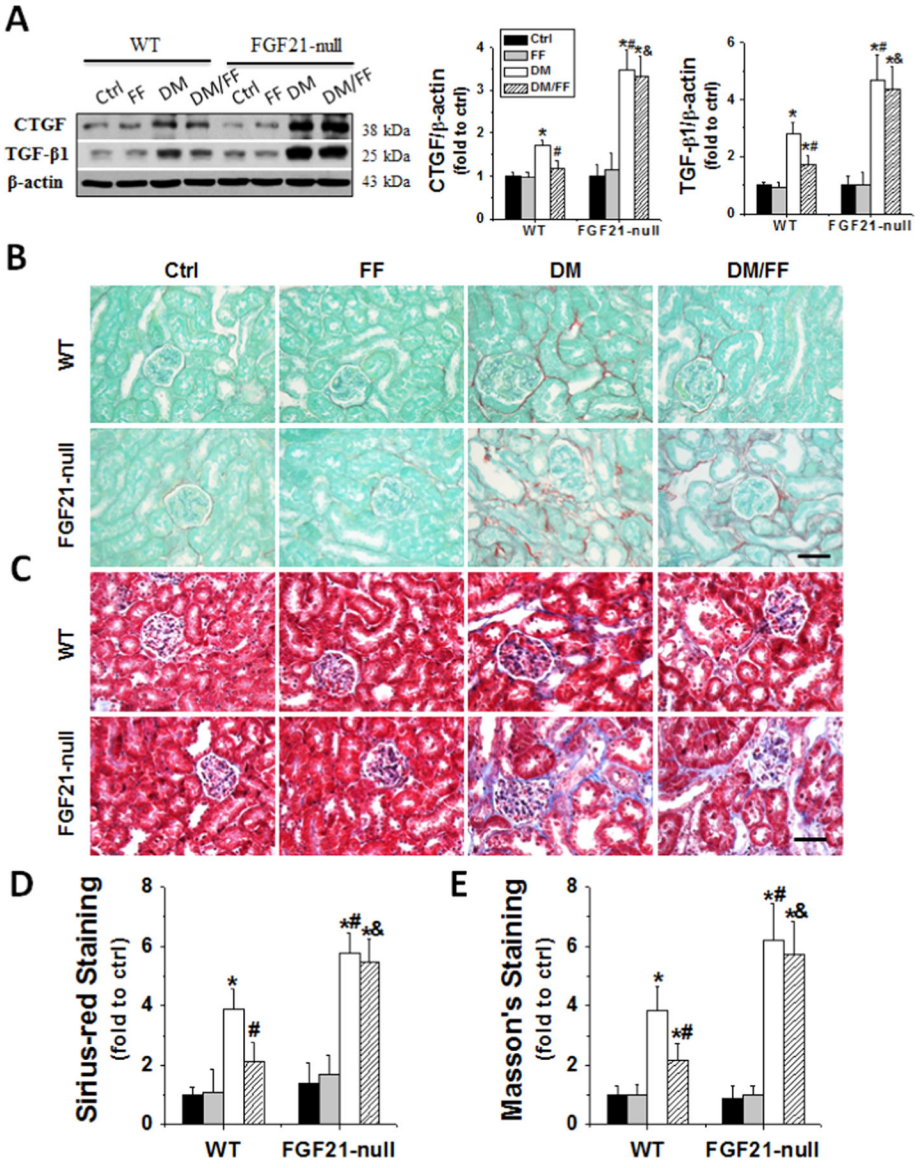

Fig. 8.

FGF21 gene deletion abolished the protective effects of FF against diabetes-induced renal fibrosis. Renal fibrosis was evaluated by the expression of CTGF and TGF-β1 with Western blot (A) and also by Sirius-red (B) (red) and Masson's (C) (blue) staining (400×, scale bare 100 μm) at 3 M after diabetes onset. Semi-quantitative analyses for Sirius-red and Masson's staining were presented as (D) and (E), respectively. Data are presented as the mean±S.D. ($n \geq 5$). * $p<0.05$ vs. WT/Ctrl; # $p<0.05$ vs. WT/DM; & $p<0.05$ vs. WT/DM/FF.

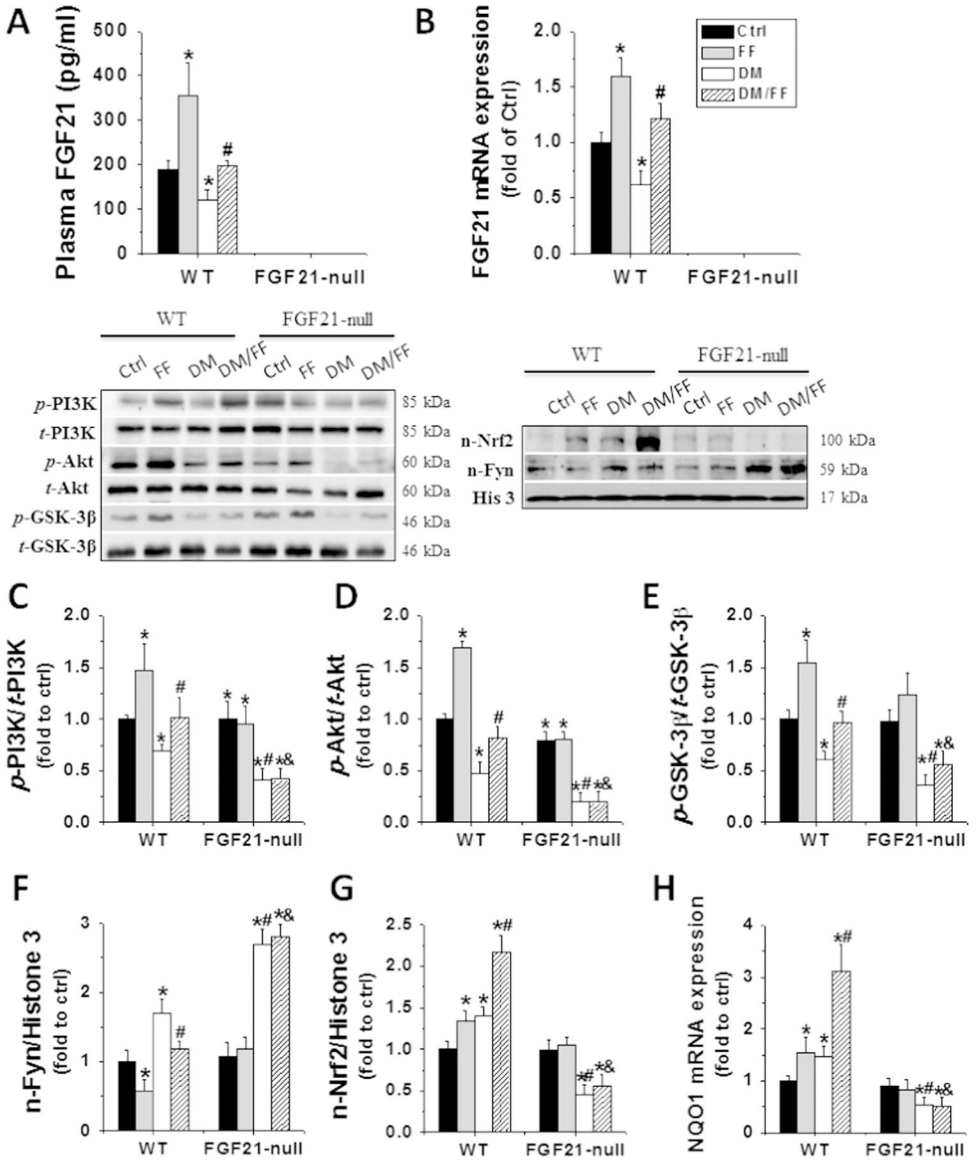

Fig. 9.

FGF21 gene deletion abolished FF-induced activation of the PI3K/Akt/GSK-3β/Fyn pathway and Nrf2 function. Renal tissues were collected at 3 M. Plasma levels (A). and renal mRNA expressions (B) of FGF21 were assessed by sandwich ELISA and qRT-PCR. Western blot was used to examine the renal expressions and activations of total and phosphorylated PI3K (C), Akt (D), and GSK-3β (E). Renal nuclear protein of Fyn (F) and Nrf2 expression (G) were examined by Western blot. The function of Nrf2 was examined by evaluating the expression of its downstream effector, NQO1, by qRT-PCR (H). Data are presented as the mean±S.D. ($n \geq 5$). * $p<0.05$ vs. WT/Ctrl; # $p<0.05$ vs. WT/DM; & $p<0.05$ vs. WT/DM/FF.

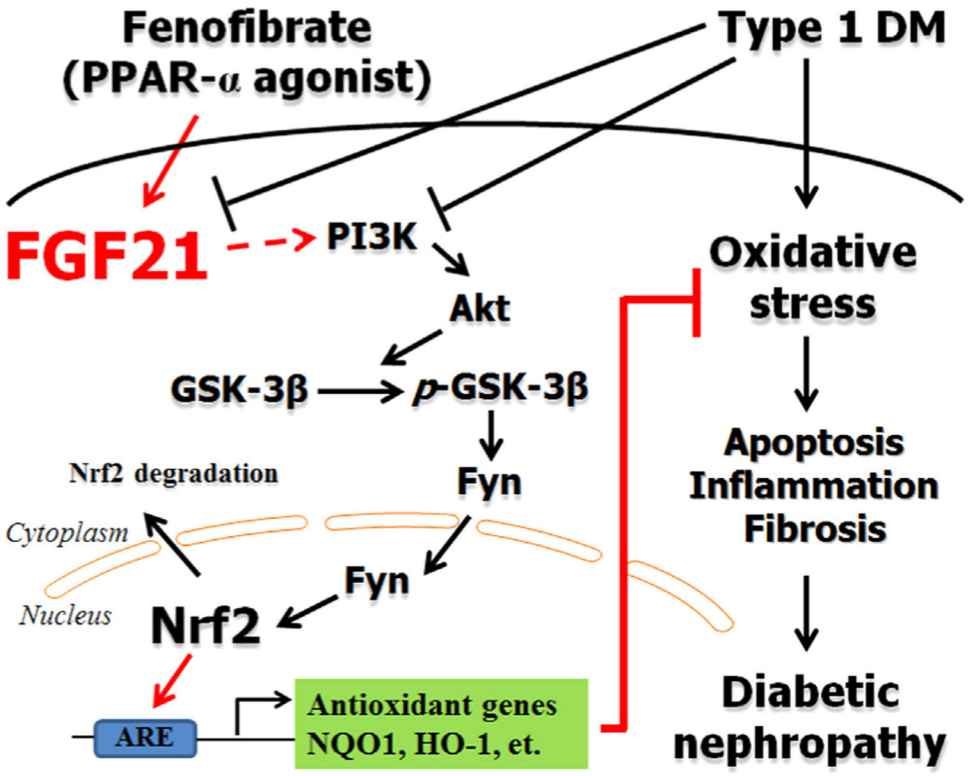

Fig. 10.

Schematic illustration for the preventive effect of FF on diabetic nephropathy. Diabetes induces renal oxidative stress, apoptosis, inflammation, and fibrosis, leading to diabetic nephropathy via increasing oxidative stress. Fenofibrate (FF) attenuates diabetes-induced the aforementioned insults to prevent diabetic nephropathy. FF-induced renal protection from diabetes is mediated by up-regulating FGF21, and this may in turn stimulates PI3K/Akt/GSK-3β/Fyn-mediated activation of the Nrf2 anti-oxidative pathway.

Table 1

Effect of FF on diabetes-induced metabolic index at 3 M and 6 M.

	Ctrl	FF	DM	DM/FF
3 M				
BW gain (g)	4.32±0.22	2.78±1.02	0.50±0.68 *	1.88±0.58 *#
BG (mg/dl)	118.2±6.55	123.4±15.97	363.2±26.78 *	307.6±34.53 *
TG (mg/dl)	48.30±15.44	42.12±11.87	120.74±16.96 *	83.80±12.66 *#
CHOL (mg/dl)	80.62±7.15	74.96±13.14	145.72±12.30 *	110.92±3.16 *#
6 M				
BW gain (g)	5.02±0.66	4.40±0.91	1.05±0.47 *	2.38±0.37 *#
BG (mg/dl)	114.3±11.61	114.7±19.88	358.6±50.86 *	357.5±37.25 *
TG (mg/dl)	52.16±13.82	41.47±10.52	152.07±12.48 *	99.04±13.07 *#
CHOL (mg/dl)	82.18±7.50	81.49±10.97	171.41±12.86 *	112.37±6.49 *#

Notes: Data are presented as the mean±S.D. ($n \geq 5$). FF: fenofibrate; BW=body weight; BG=blood glucose; TG=triglyceride; CHOL=cholesterol.

* $p<0.05$ vs. corresponding Ctrl.

# $p<0.05$ vs. corresponding DM.

Table 2

Effect of FF on diabetes-induced metabolic index in FGF21-null and WT mice.

	Ctrl	FF	DM	DM/FF
WT				
BW gain (g)	4.53±1.38	2.95± 1.15	0.10±1.07 *	2.3470.87 *#
BG (mg/dl)	117.0±23.26	124.0±24.51	361.0±26.23 *	353.5728.41 *
TG (mg/dl)	43.27±7.35	35.02±10.72	129.86±20.83 *	80.02714.85 *#
CHOL (mg/dl)	66.93±18.15	62.52±18.14	191.01±28.30 *	119.10722.16 *#
FGF21-null				
BW gain (g)	6.30±0.74	4.93±0.99	1.59±0.95 &	1.05±0.85 &
BG (mg/dl)	130.3±24.76	120.3±22.04	383.5±54.03 &	369.8±42.01 &
TG (mg/dl)	44.09±7.76	43.83±18.25	175.42±25.94 &	115.37±22.28 &†
CHOL (mg/dl)	78.48±11.50	79.09±19.97	266.33±43.86 &	178.34±25.49 &†

Notes: Data are presented as the mean±S.D. ($n \geq 5$). FF: fenofibrate; BW=body weight; BG=blood glucose; TG=triglyceride; CHOL=cholesterol.

* $p<0.05$ vs. WT/Ctrl.

\# $p<0.05$ vs. WT/DM.

& $p<0.05$ vs. FGF21-null/Ctrl.

† $p<0.05$ vs. FGF21-null/DM.